

---

# Determining the Arrival Time Delay of Galactic Core-collapse Supernova Neutrino Burst at Different Neutrino Experiments

---

Leung Ching Yu, Otto  
Mentor: Prof. Jeff Tseng

*The Department of Physics, The Chinese University of Hong Kong*  
*The Sub-department of Particle Physics, University of Oxford*

December 25, 2023

## Abstract

Triangulation pointing to galactic core-collapse supernovae requires information about the arrival time delay of neutrino burst at different neutrino experiments. This report presents a new model-independent approach to determine the arrival time delay using binned time series analysis and maximum-likelihood method. It is a modified approach based on the cross-covariance method proposed in the working paper of Prof. Jeff Tseng and Dr. Farrukh Azfar. To compare the performance of the new method with other proposed methods, supernova neutrino signals without background are generated. Under particular condition, the new approach outperforms cross-covariance approach while all the methods being tested have comparable bias and uncertainty under practical conditions. Further error analyses with background neutrino signal are required.

# 1 Introduction

Galactic core-collapse supernova (CCSN) are extremely rare ( $1.63 \pm 0.46$  per century in the Milky Way) but of utmost importance to reveal the physics of massive stars [1]. Supernova Early Warning System (SNEWS) was designed to provide CCSN alert, including its sky location, before the EM radiation burst arrives the Earth [2]. By pointing telescopes to the location in advance, we can hopefully capture all the critical information from the EM radiation burst. The neutrino burst from SNe plays an important role here as it arrives the earth earlier than the EM radiation.

Triangulation pointing, which makes use of neutrino burst time delay at different experiments, is one of the approaches to determine the sky location of SNe [3]. Previous study developed the Chi-square method to determine the time delay between two experiments [4]. However, the uncertainty of the time delay is obtained by running MC trials, which require a specific model describing the neutrino light-curve. Given that the shape of the light-curves can be very different under different circumstances, a model-dependent approach is not preferable. Running MC trials is time consuming as well.

This project presents a new model-independent approach, namely modified cross-covariance, using binned time series analysis and maximum-likelihood method based on the cross-covariance method proposed in the working paper of Prof. Jeff Tseng and Dr. Farrukh Azfar. Performances of the new method together with other proposed methods were evaluated when no neutrino background signal was presented.

## 2 Theory

### 2.1 Triangulation Pointing

The time delay  $\tau$  between two neutrino detectors are defined by [2]

$$\tau = \vec{d} \cdot \frac{\vec{n}}{c} \quad (1)$$

where  $\vec{d}$  is the vector connecting the location of two detectos and  $\vec{n}$  is the unit vector pointing from the CCSN to the

earth.  $\vec{n}$  can be expressed as the following [4]:

$$\vec{n} = (-\cos(\beta - \gamma)\cos\delta, -\sin(\beta - \gamma)\cos\delta, -\sin\delta) \quad (2)$$

where  $\beta$  is the right ascension,  $\delta$  is the declination of the CCSN and  $\gamma$  is the Greenwich mean sidereal time of the event.

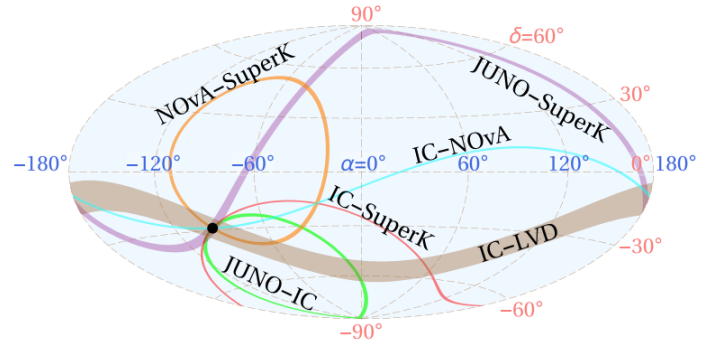


Figure 1: Sky location with  $1\sigma$  confidence level adopted from Ref. [5]. The black dot, where all the rings overlap, shows the actual SN location.

With known time delay, each pair of detectors should give us a ring of sky location with thickness related to the uncertainty  $\delta\tau$  as shown in figure 1.

## 3 A Summary of the Working Paper

The working paper has proposed two model-independent approaches to determine the time delay  $\tau$  between two neutrino detectors, namely cross-covariance approach and double Poisson likelihood approach. However, both approaches have their own issues.

### 3.1 Cross-covariance Approach

The cross-covariance function is defined as

$$R_c(\tau) = \frac{1}{N} \sum_{j=1}^N n_j m_j(\tau). \quad (3)$$

where  $N$  is the number of time bin,  $n_j$  is the events yield inside  $j$ -th time bin of the reference detector which is centered at  $t_j$  and  $m_j$  is the event yield inside  $j$ -th time bin of another detector which is centered at  $t_j + \tau$ . The best time delay can be obtained by maximizing this function. The paper found that maximizing the function is equivalent to maximizing the following likelihood under some approximations

$$L = \prod_{j=1}^N \frac{1}{\sqrt{2\pi}\sigma} e^{-\frac{1}{2} \frac{(n_j - \frac{m_j - c}{\alpha} - b)^2}{\sigma^2}} \quad (4)$$

where  $b$  and  $c$  are the expected background of the two detectors,  $\alpha$  is the ratio of the expected yields of two detectors and  $\sigma$  is the uncertainty which is approximated to be constant under different time bin. This approximation induces significant bias for time bin width larger than 100ms.

### 3.2 Double Poisson Likelihood Approach

The likelihood after marginalizing over the expected yields in each bin  $\mu_j$  is

$$L = \prod_{j=1}^N \int_0^\infty \frac{(\mu_j + b)^{n_j} e^{-\mu_j - b} (\alpha \mu_j + c)^{m_j} e^{-\alpha \mu_j - c}}{n_j! m_j!} d\mu_j \quad (5)$$

The best time delay is obtained by maximizing Equation 5. If we assume no background in both detectors, it becomes

$$L = \prod_{j=1}^N \frac{(n_j + m_j)!}{n_j! m_j!} \frac{\alpha^{m_j}}{(\alpha + 1)^{n_j + m_j + 1}} \quad (6)$$

The main issue lies in solving the integral in Equation 5 when detectors have non-negligible background signal. Despite many numerical methods of solving integral, they are time consuming.

The working paper has shown that the integral can be transformed into

$$\frac{\alpha^{m_j} e^{\alpha b - c}}{n_j! m_j!} \sum_{i=0}^{m_j} \binom{m_j}{i} \frac{(\frac{c}{\alpha} - b)^i}{(1 + \alpha)^{n_j + m_j - i + 1}} \Gamma(n_j + m_j - i + 1, b(1 + \alpha)) \quad (7)$$

However, calculating the value of the series is computationally intensive as well. As the alert system requires a fast response time, a time consuming approach is not appropriate.

## 4 Modified Cross-covariance Approach

In the light of the above, I modified the cross-covariance approach using a novel approximation to Poisson distribution so that the change of uncertainty in different bin is taken into account.

### 4.1 Approximation to Poisson Distribution

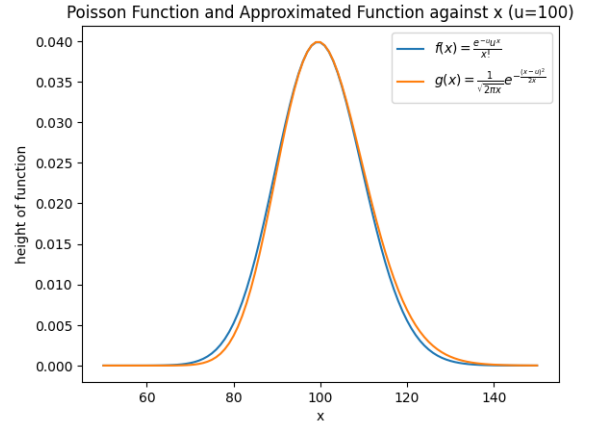


Figure 2: Poisson function and approximated function against  $x$  with  $u$  equal to 100.

I first approximate the Poisson distribution to Normal distribution without continuity correction so that

$$f(x, u) = \frac{e^{-u} u^x}{x!} \approx \frac{1}{\sqrt{2\pi u}} e^{-\frac{(x-u)^2}{2u}} \quad (8)$$

where  $x$  is the Poisson variable and  $u$  is the expected value

of  $x$ . Then, I replace the uncertainty  $u$  by its estimator  $x$  and obtain

$$f(x, u) = \frac{e^{-u}u^x}{x!} \approx \frac{1}{\sqrt{2\pi x}} e^{-\frac{(x-u)^2}{2x}} \quad (9)$$

The Poisson function and the approximated function look similar if we plot them against  $x$  as shown in figure 2. It was observed that the larger  $u$  is, the more similar they are.

One may want to extend the above approximation to the case that expected value of  $x$  is  $au + k$  instead of  $u$ . If we consider the 3D space formed by  $x$ ,  $u$  and the function itself, this is simply shifting the two surfaces by  $k$  to the negative  $u$  direction and compress them along the  $u$  direction by a scale of  $a$ . As long as the two function looks similar, the transformation does not matter.

## 4.2 Derivation

Following is the derivation of the likelihood of modified cross-covariance approach. To begin with, the event yields in time bin  $j$   $n_j$  and  $m_j$  are variables following Poisson distribution, i.e.

$$n_j \sim \text{Poi}(\mu_j + b) \quad m_j \sim \text{Poi}(\alpha\mu_j + c) \quad (10)$$

Using the above approximation, it becomes

$$n_j \sim N(\mu_j + b, \sqrt{n_j}) \quad m_j \sim N(\alpha\mu_j + c, \sqrt{m_j}) \quad (11)$$

This implies

$$n_j = \mu_j + b + \epsilon_{n_j} \quad m_j = \alpha\mu_j + c + \epsilon_{m_j} \quad (12)$$

where  $\epsilon_{n_j} \sim N(0, \sqrt{n_j})$  and  $\epsilon_{m_j} \sim N(0, \sqrt{m_j})$ .

To eliminate  $\mu_j$ , we combine Equation 12 into

$$n_j = \frac{m_j - c}{\alpha} + b + \epsilon_{k_j} \quad (13)$$

where  $\epsilon_{k_j} \sim N(0, \sqrt{n_j + \frac{m_j}{\alpha}})$

The likelihood in each time bin can be expressed as

$$L_j = P(n_j, m_j | \tau; \alpha, b, c) \quad (14)$$

The probability can be broken into a product of two terms, i.e.

$$P(n_j, m_j | \tau; \alpha, b, c) = P(n_j | \tau; \alpha, b, c, m_j) P(m_j | \tau; \alpha, b, c) \quad (15)$$

Since  $\tau, \alpha, b$  and  $c$  do not provide any information about  $m_j$ , we approximate  $P(m_j | \tau; \alpha, b, c)$  to be flat while we express  $P(n_j | \tau; \alpha, b, c, m_j)$  using Equation 11. The likelihood in each time bin becomes

$$L_j = \frac{1}{\sqrt{2\pi(n_j + \frac{m_j}{\alpha})}} e^{-\frac{1}{2} \frac{(n_j - \frac{m_j - c}{\alpha} - b)^2}{n_j + \frac{m_j}{\alpha}}} \quad (16)$$

Including all time bin and taking the log, we obtain

$$\log L = -\frac{1}{2} N \log(2\pi) - \frac{1}{2} \sum_{j=1}^N \left( \log(n_j + \frac{m_j}{\alpha}) + \frac{(n_j - \frac{m_j - c}{\alpha} - b)^2}{n_j + \frac{m_j}{\alpha}} \right) \quad (17)$$

Maximizing  $\log L$  is equivalent to maximizing the function

$$R_p(\tau) = - \sum_{j=1}^N \left( \log(n_j + \frac{m_j}{\alpha}) + \frac{(n_j - \frac{m_j - c}{\alpha} - b)^2}{n_j + \frac{m_j}{\alpha}} \right) \quad (18)$$

Hence, the best time delay is obtained by maximizing Equation 18.

## 4.3 Uncertainty Estimation

With the log likelihood scan, we can derive the uncertainty of the best time delay easily, which can be compared to the one obtained from MC trials.

Since figure 3 shows that  $\tau$  follows an unimodal distribution, we approximate the log likelihood by a second order

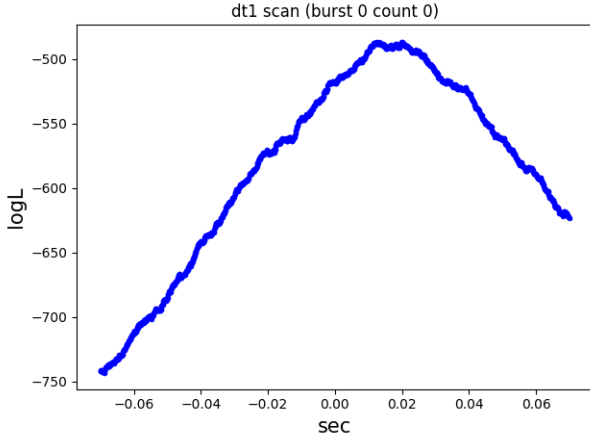


Figure 3: Modified cross-covariance log likelihood as a function of  $\tau$  using SNO+ and SK with total event yields 5000 and 10000 respectively. The actual time delay is 14.66ms

polynomial of  $\tau$ . In other words, we approximate the likelihood (not the log one) to a Gaussian function of  $\tau$ . Since taking the log and then the second derivative of a Gaussian function at the peak gives the negative reciprocal of variance, we can estimate the uncertainty by taking the second derivative of the second order polynomial with respect to  $\tau$  at the peak.

## 5 Error Analysis without Background

I evaluated the dependence of bias and RMS on different variables, including true time delay, time window, time bin width, SNe models and events yields of detectors, of the three proposed approaches: cross-covariance, modified cross-covariance and double Poisson likelihood. In the following, I assumed no background in both detectors SNO+ and SK, and SK was chosen to be the reference detector. For each data point, I ran 1000 trials with  $\tau$  tested from  $+70ms$  to  $-70ms$ . By considering the diameter of the earth,  $\tau$  must be within  $\pm 40ms$ . However, if  $\tau$  is constrained within the physical region, some of the trials may accumulate on the boundaries. We can either neglected these trials or further extend boundaries. I opted for the latter solution because I had a better understanding of the meaning of bias and RMS obtained this way. Neglecting unphysical trials simply means neglecting those strongly affected by signal fluc-

tuations. Then, the meaning of RMS here is a bit vague because it only reveals part of the effect.

As shown in figure 4, except the two orange lines in the cross-covariance graphs corresponding to 200ms time bin width, all methods has constant bias and RMS under different true time delay regardless of the time bin width and time window. It is as expected because true time delay only affects the amount of time the program need to shift the light-curve before best time delay is attained. As long as the shape of both light-curves remains the same, bias and RMS are unaffected.

To understand the two special cases, I looked at the distribution of the 1000 best time delay and the log likelihood scan of one of the trials of cross-covariance as shown in figure 5. The fact that majority of trials accumulate on both sides and the log likelihood scan does not attain a local maximum implies the failure of the method. As mentioned, due to the constant uncertainty approximation, the method fails when time bin width is larger than 100ms. Under this condition, modified cross-covariance approach successfully address the issue and outperforms cross-covariance approach.

As a result, I neglected these two lines and concluded that bias and RMS of all methods are invariant with true time delay i.e. the choice of detectors, the position and time of SNe. I also plotted these graphs with other yields (2000 and 5000) and another model (nubar-e-LS220-s40.0c-bh). The same conclusions were drawn.

It is observed that using different time window may affect the result by varying degrees, depending on the model and event yields. Generally, as long as we use certain time bin width, choosing 5s and 10s time window does not affect much. For example, for 20ms time bin width, bias and RMS differ by less than 0.5ms and 1ms respectively under different model for all the methods.

Next, we would like to evaluate the effect of time bin width.

As expected, time bin width between 0ms to 20ms has the least bias for the three methods as shown in figure 6 since the range is roughly the time scale of SNe. Among the four data points in between (1ms, 2ms, 10ms and 20ms time bin width), 20ms data point has the least RMS value. I also plotted the graphs using other event yields (400 and 10000) and model (nubar-e-ls220-s40.0c-bh), which shows similar behaviour.

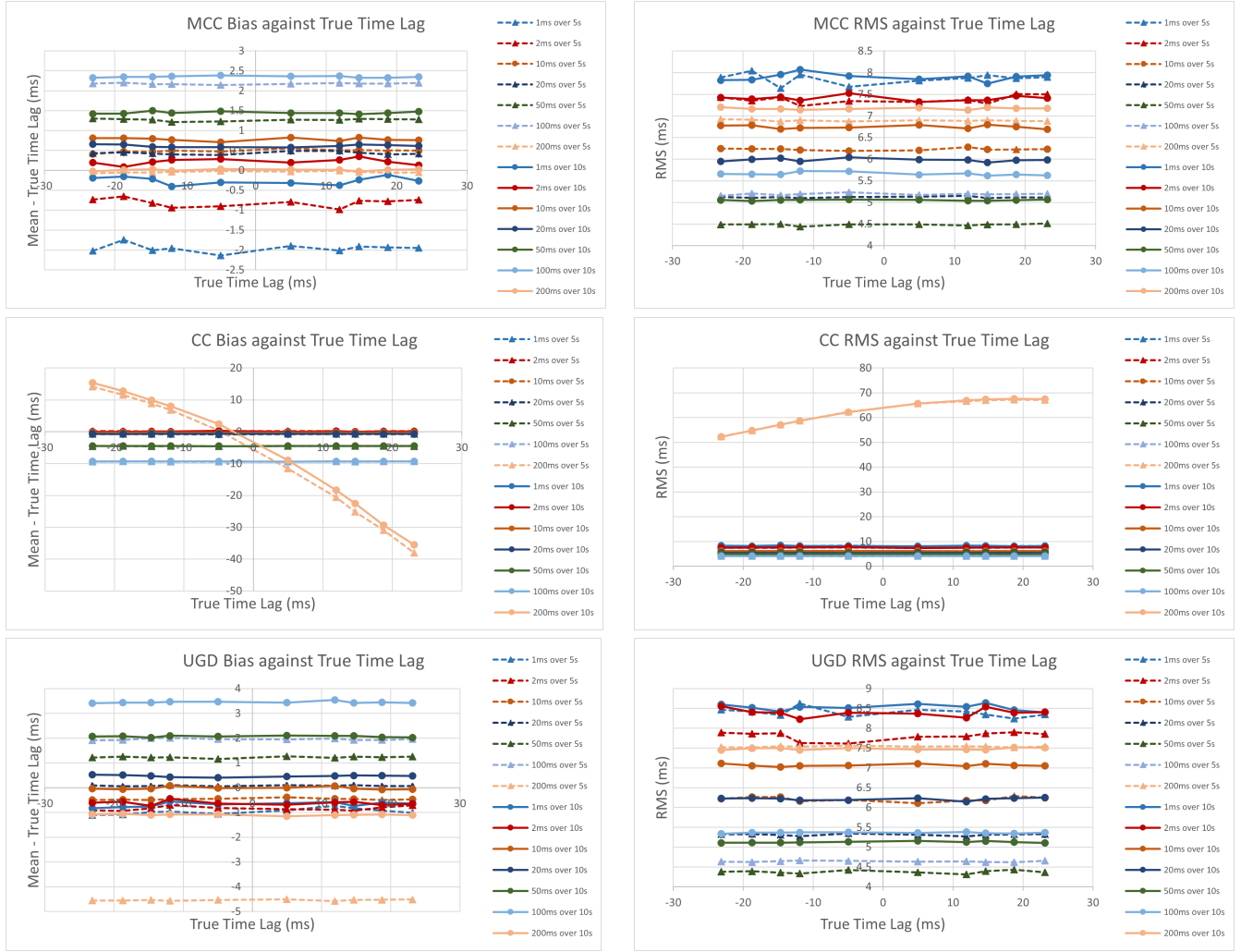


Figure 4: Bias (left column) and RMS (right column) as a function of true time delay for SNO+ and SK, with 2000 and 10000 events, using model nubar-e-LS220-s27.0co.data. The methods, from the top to the bottom, are as follows: modified cross-covariance, cross-covariance and double Poisson likelihood. Each line represents a specific combination of time bin width and time window

The only variables left to be tested are SN models and event yields, which were evaluated together.

In the following, the time delay  $\tau$  was tested from +140ms to -140ms. As we decrease the event yields, the 1000 best time delay trend to distribute more uniformly. A wider range of time delay is therefore necessary to avoid data points piling up on the boundaries. Besides, switching reference detector should not affect bias and RMS theoretically as it simply flips the sign of the true time delay, of which bias and

RMS are independent. In practice, it actually affects bias and RMS somehow when the two detectors observe different event yields. To make the following graph symmetric, I chose the detector with the largest event yields as reference instead of fixing SK. As 20ms time bin width has a relatively small bias and the least RMS, I plotted the following graph using this time bin width and 5s time window.

Figure 7 shows the three dimensional plots of bias (left) and RMS (right) versus SNO+ event yields versus SK event

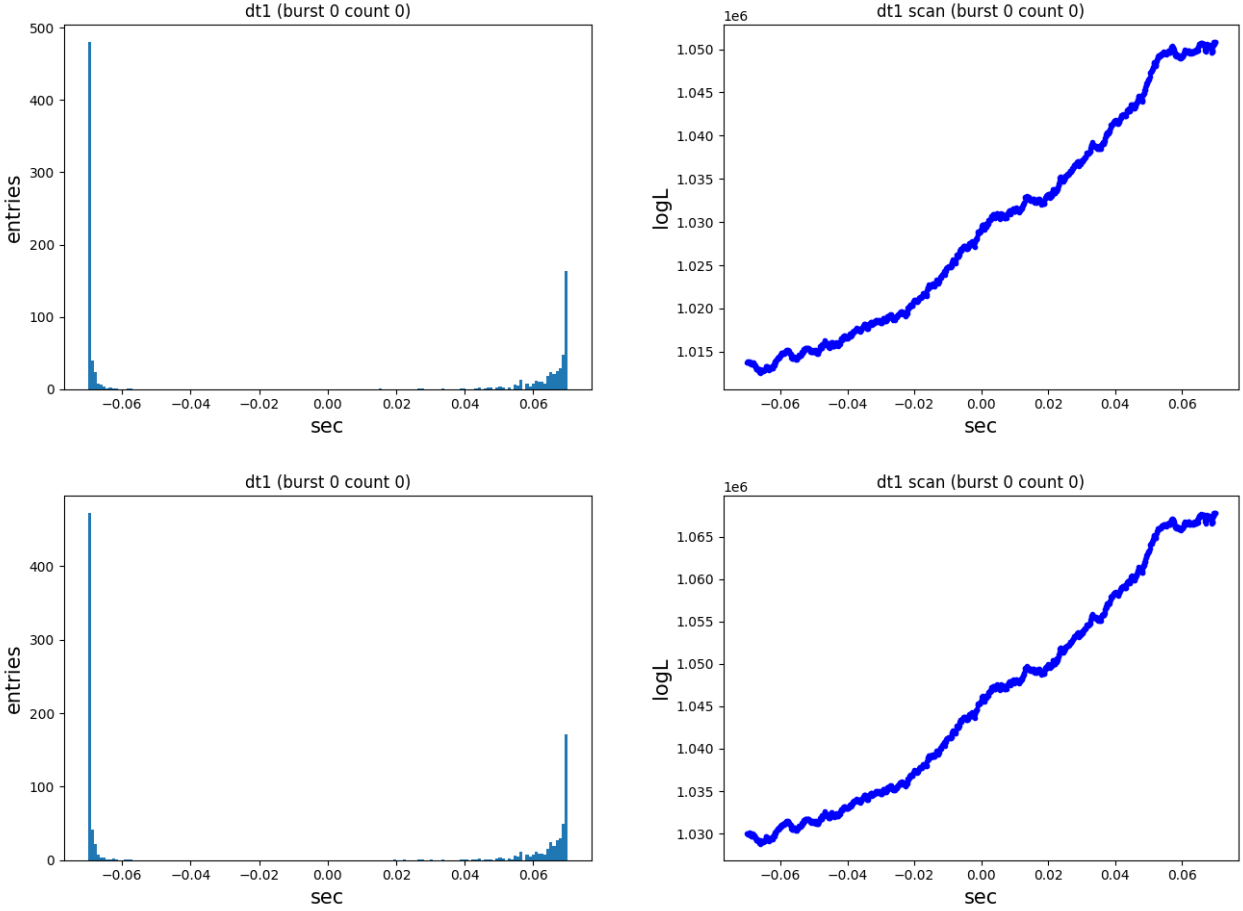


Figure 5: Left: distribution of 1000 best time delay of cross-covariance method with 200ms time bin width and 14.66ms true time delay. Right: log likelihood scan of time delay of cross-covariance method with 200ms time bin width and 14.66ms true time delay. Top: 5s time window. Bottom: 10s time window

yields of the three approaches. As expected, both bias and RMS are symmetric, which would not be the case if we fixed SK as reference.

All three methods behave similarly. Generally, bias surfaces hunch up on the edge and becomes flat as event yield increases, and bias goes to negative when event yields of both detectors are small. Besides, bias increases with relative yields. It is suggested that approximations used to derive the likelihood induce bias, but the behaviour is not well understood. Regarding RMS, since the larger the event yields they are, the more information is provided, the uncertainty of all methods decreases. It is observed that using different models may slightly affect bias but not RMS because RMS

mainly depends on event yields.

All these methods have comparable bias and RMS when event yields are large (greater than 2000 events). When event yields are small ( $\sim 50$  events), modified cross-covariance has slightly smaller bias than the other two methods.

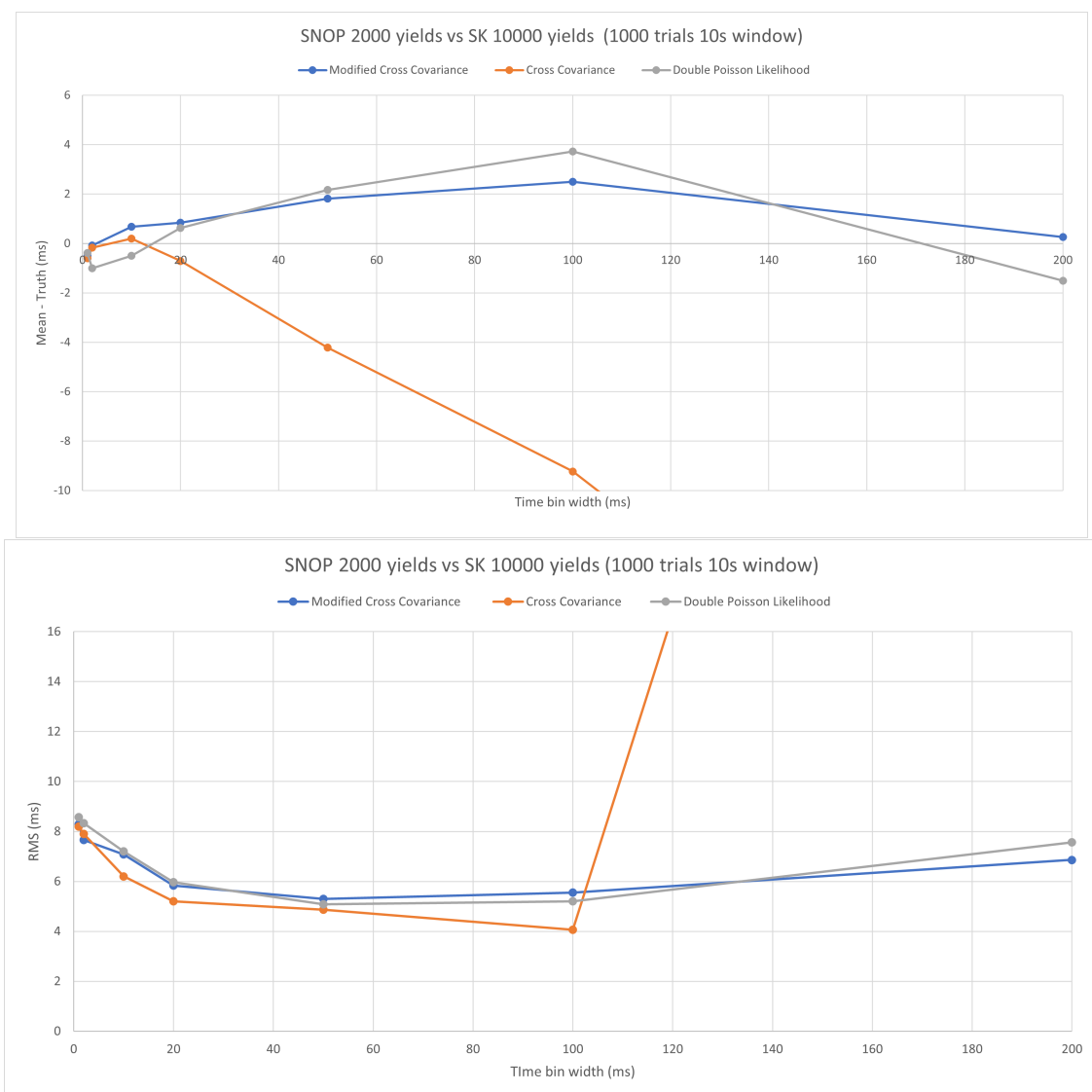


Figure 6: Bias (top) and RMS (bottom) as a function of time bin width for SNO+ and SK, with 2000 and 10000 events, at 14.66ms true time delay using 10s time window and model nubar-e-LS220-s27.0co.data

## 6 Future Work

of event yields

- Doing error analyses with background signal

Followings need to be done in the future:

- Understanding why switching reference detector affects bias and RMS
- Understanding the behaviour of bias
- Searching for an expression for bias and RMS in terms



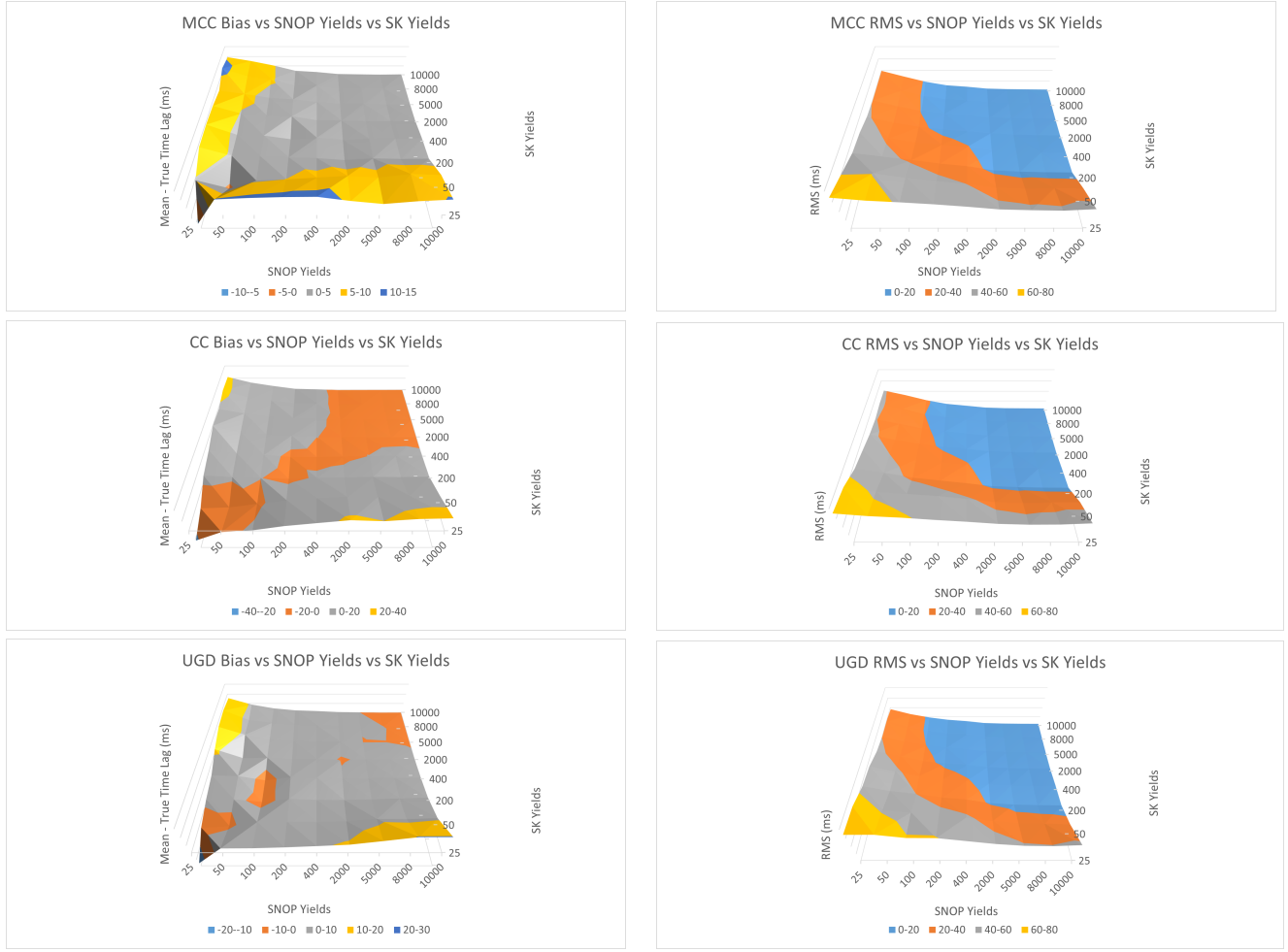


Figure 7: Bias (left) and RMS (right) as a function of event yields of SNO+ and SK using model nubar-e-LS220-s27.0co.data. The methods, from the top to the bottom, are as follows: modified cross-covariance, cross-covariance and double Poisson likelihood.

## 7 Conclusions

Modified cross-covariance approach was developed. It takes advantages of cross-covariance method while it does not make use of the constant uncertainty approximation. When background signal is included, the likelihood can be computed much faster than the double Poisson likelihood.

The performance of cross-covariance, modified cross-covariance and double Poisson likelihood were evaluated when no background was presented. The following conclusions were drawn when 20ms time bin width was used, which has a relatively small bias and the least RMS under

different conditions. Event yields are the variables that affect bias and RMS the most while time window and choice of SN models have a minor effect on bias and RMS. All three methods have comparable bias and RMS, but modified cross-covariance has slightly smaller bias when event yields are small.

## 8 Acknowledgements

I would like to show my deepest gratitude to Prof. Jeff Tseng, Dr. Farrukh Azfar and SNO+ team from Oxford University, who guided me throughout the project and provided valuable opinions and inspiring ideas.

I am also very grateful for the financial support provided by Fung Scholarship, Professor Charles K. Kao Research Exchange Scholarship, CN Yang Research Scholarship, Yasumoto International Exchange Scholarship and Reaching Out Award.

Last but not least, I would like to thank the department of physics at Chinese University of Hong Kong and the particle physics sub-department at Oxford University for organizing the exchange program.

## 9 References

- [1] Karolina Rozwadowska, Francesco Vissani, and Enrico Cappellaro. On the rate of core collapse supernovae in the milky way. *New Astronomy*, 83:101498, 2021.
- [2] S Al Kharusi, SY BenZvi, JS Bobowski, W Bonivento, V Brdar, T Brunner, E Caden, M Clark, A Coleiro, M Colomer-Molla, et al. Snews 2.0: a next-generation supernova early warning system for multi-messenger astronomy. *New Journal of Physics*, 23(3):031201, 2021.
- [3] T Mühlbeier, H Nunokawa, and R Zukanovich Funchal. Revisiting the triangulation method for pointing to supernova and failed supernova with neutrinos. *Physical Review D*, 88(8):085010, 2013.
- [4] Alexis Coleiro, M Colomer Molla, Damien Dornic, Massimiliano Lincetto, and Vladimir Kulikovskiy. Combining neutrino experimental light-curves for pointing to the next galactic core-collapse supernova. *The European Physical Journal C*, 80(9):856, 2020.
- [5] Vedran Brdar, Manfred Lindner, and Xun-Jie Xu. Neutrino astronomy with supernova neutrinos. *Journal of Cosmology and Astroparticle Physics*, 2018(04):025, 2018.